Metal Strip Grating on Grounded Dielectric Slab and PEC/PMC Shielded Interconnect: Modal Relationships

Kun Chen [1], Jiming Song [1], and Telesphor Kamgaing [2]

[1] Department of Electrical and Computer Engineering
Iowa State University, Ames, IA 50011, USA
{kunc, jisong}@iastate.edu

[2] Intel Corporation, Chandler, AZ 85226, USA
telesphor.kamgaing@intel.com

Abstract ― This paper employs the spectral domain approach for full wave analysis of metal strip grating on grounded dielectric slab and microstrips shielded with either Perfect Electric Conductor (PEC) or Perfect Magnetic Conductor (PMC) walls. The modal relations between these structures are revealed by exploring their symmetries. It is derived analytically and validated numerically that all the even and odd modes of the latter two (when they are mirror symmetric) find their correspondence in the modes of metal strip grating on grounded dielectric slab when the phase shift between adjacent two unit cells is 0 or π. Extension to non-symmetric case is also made. Several factors, including frequency, grating period, slab thickness and strip width, are further investigated for their impacts on the effective permittivity of the dominant mode of PEC/PMC shielded microstrips. It is found that the PMC shielded microstrip generally has a larger wave number than the PEC shielded microstrip.

Index Terms ― Grounded dielectric slab, metal strip grating, perfect electric conductor, perfect magnetic conductor, periodic boundary condition, shielded microstrip.

I. INTRODUCTION

In modern integrated circuits, interconnects play such an important role that accurate and efficient modeling of them is a must. For example, COMS circuits see the responsibility of interconnects for more than half of the on-chip capacitance and dynamic power dissipation, significant delay to critical paths, and noise and jitter to signals [1]. However, there are many challenges in successful modeling of interconnects: firstly, the state-of-the-art 3D circuits usually come as multilayered structures, the modeling of which is quite involved [2]; secondly, high density of integration leads to millions of interconnects within a very limited space; thirdly, high frequency means we can no longer take neglect of conduction loss and metal thicknesses as granted.

Faced with such a complexity, it is natural and beneficial for us to abstract some key features of the interconnects and give priorities to some typical structures, as this simplifies the problem and allows for the employment of reliable simulation techniques. The study of multilayered structure can be considered the generalization of the single layered structure. Also, many layouts of interconnects are well approximated with periodic structures. In this work, we consider the single layered microstrip with PEC/PMC walls as well as Metal Strip Grating on Grounded Dielectric Slab (MSG-GDS).

Microstrip transmission lines, as we know, are key building blocks for interconnects. Microstrips shielded with Perfect Electric Conductors (PECs) draw attention in that they can model the effect of packaging such as providing isolation between different elements as well as mechanic support for the integrated circuit [3]. As a dual of the PEC shielded case, the Perfect Magnetic Conductor

Submitted On: February 5, 2014
Accepted On: September 6, 2014

(PMC) shielded microstrip is also worth investigation. Metal Strip Grating on Grounded Dielectric Slab (MSG-GDS), which is a grounded dielectric slab loaded with one-dimensional periodic metal strips, is another classic structure which has seen various applications in electronic engineering. For instance, the behaviors of the waves travelling in the direction perpendicular to the strips are utilized to design leaky wave antennas [4]. Strip-element phased arrays [5] and polarizers with low cross-polarization [6] also account for some important applications of MSG-GDS. In fact, we can treat the three structures mentioned above as only one: a microstrip, but with different boundary conditions. It is not unfamiliar to us that the PEC and PMC boundary conditions are used to truncate the simulation domain or analyze periodic structures in high frequency electromagnetic field solvers. But what exactly is the relationships between the PEC, the PMC and the periodic boundary conditions? Though for each of these structures, there exists an abundance of literatures, it is hardly seen in the literature an explicit elaboration of this relation. As far as we are concerned, only the literature [7] bears a short discussion about the relationships between the modes of the PEC/PMC shielded microstrips and the MSG-GDS, but it is restricted to the case in the absence of phase shift between adjacent periods.

Based on our previous work [8], we aim in this paper to reveal more comprehensively the modal relationships between MSG-GDS and the PEC/PMC shielded microstrips. To this end, we perform a full wave analysis for these structures using the spectral domain approach [9]. Two variations of these structures will be considered: one with a top PEC shield, and the other without, as illustrated in Fig. 1 (a) and (b). We first consider the structures when they are symmetric, then extensions to non-symmetric ones are carried out. Furthermore, we also look at the impacts of frequency, grating period and slab thickness on the wave number of the dominant mode of PEC/PMC shielded microstrips. Numerical results are presented to validate our conclusions.

II. SPECTRAL DOMAIN APPROACH

The MSG-GDS is drawn in Fig. 1 (a). The structure obtained by adding a top PEC shield, illustrated in Fig. 1 (b), will be considered together. A coordinate system is created in Fig. 1 (c), added with some assisting dash lines locating symmetry planes. As shown in the figure, a dielectric slab of thickness h is grounded by an infinite PEC plane, and topped by a grating (with period P) of perfect conducting strips of widths w. We assume that the thickness of the metal strips is zero. The permittivity and permeability for the slab are ε_1 and μ_1, and for the region above the slab are ε_2 and μ_2. If there is a top shield, the distance to the top slab surface is d. The shielded microstrips can be obtained by placing PEC (or PMC) walls at $x=\pm P/2$, so we save their illustrations for book-keeping. For the MSG-GDS, the waves can be guided in arbitrary horizontal directions, but we focus on the case when the wave propagates along the strips.

The spectral domain approach [9] is a very accurate and efficient method to solve the eigenproblem for microstrip structures, hence, it will be adopted in this work. Given the periodicity of the structure, the Floquet theorem enables us to confine our scope to the first unit cell (between $x=\pm P/2$). The tangent electric fields at the top surface of the slab can be determined by the current on the metal strip and expressed in the form of a Fourier series as:

$$\sum_{n=-\infty}^{\infty}\sum_{s}\tilde{G}_{rs}(k_{xn},k_y;h)\tilde{J}_s(k_{xn})e^{-jk_{xn}x}=E_r(x,h), \qquad (1)$$

where k_{xn} and k_y are the wave numbers in x and y directions, with the Bloch wave number $k_{xn}=(\phi_0+2n\pi)/P$ ($n\in Z$), where ϕ_0 is the phase shift between adjacent periods, $r,s\in\{x,y\}$, $\tilde{J}_s$ is the Fourier transform of the current in the unit cell, $\tilde{G}_{rs}$ is the spectral dyadic Green's function available in simple analytic form [9]:

$$\begin{aligned}
\tilde{G}_{xx}(k_{xn},k_y) &= j\eta_2(k_2\Delta)^{-1}[\mu_r\gamma_1(k_{xn}^2-k_2^2)\tanh(\gamma_1 h)\\
&\quad +\gamma_2(k_{xn}^2-k_1^2)\Theta]\\
\tilde{G}_{xy}(k_{xn},k_y) &= \tilde{G}_{yx}(k_{xn},k_y)= j\eta_2 k_{xn}k_y(k_2\Delta)^{-1}\\
&\quad \times[\mu_r\gamma_1\tanh(\gamma_1 h)+\gamma_2\Theta]\\
\tilde{G}_{yy}(k_{xn},k_y) &= j\eta_2(k_2\Delta)^{-1}[\gamma_1\mu_r(k_y^2-k_2^2)\tanh(\gamma_1 h)\\
&\quad +\gamma_2(k_y^2-k_1^2)\Theta], \qquad (2)
\end{aligned}$$

with

$$\Delta=[\gamma_1\coth(\gamma_1 h)+\mu_r\gamma_2\Theta^{-1}][\gamma_1\tanh(\gamma_1 h)+\varepsilon_r\gamma_2\Theta], \quad (3)$$

where we have $\varepsilon_r=\varepsilon_1/\varepsilon_2$, $\mu_r=\mu_1/\mu_2$, $\eta_i=\sqrt{\mu_i/\varepsilon_i}$, $k_i=\omega\sqrt{\mu_i\varepsilon_i}$ and $\gamma_i=\sqrt{k_{xn}^2+k_y^2-k_i^2}$, $\Theta=1$ for Fig. 1 (a) and $\Theta=\tanh(\gamma_2 d)$ for Fig. 1 (b). When $\gamma_2 d>9$, which is approximately guaranteed when $d>3P/2$, the two Green's functions has little difference if single precision is used. Since the Green's functions for the two cases are so close, they can be handled together. Then we apply Galerkin's method to solve (1), which leads us eventually to the following homogeneous linear system:

$$\begin{bmatrix} K^{xx} & K^{xy} \\ K^{yx} & K^{yy} \end{bmatrix}\begin{bmatrix} A \\ B \end{bmatrix}=\mathbf{0}, \quad (4)$$

where $K^{rs}(r,s\in\{x,y\})$ is a matrix with elements given by:

$$K_{pq}^{rs}=\sum_{n=-\infty}^{\infty}\tilde{J}_{rp}(-k_{xn})\tilde{J}_{sq}(k_{xn})\tilde{G}_{rs}(k_{xn},k_y), \quad (5)$$

where $p=1,\cdots N_x$, $q=1,\cdots N_y$ (N_x and N_y are the number of basis functions for J_x and J_y), $\tilde{J}$ is the Fourier transform of the current basis function, for which we have chosen the Chebyshev polynomials of the first and second kind for J_y and J_x respectively [10]. $A=[A_1,\cdots A_{N_x}]^T$, $B=[B_1,\cdots B_{N_y}]^T$ are the unknown expansion coefficients for J_x and J_y. To solve the eigenvalue problem, we require vanishing of the determinant of the matrix in (4). In general, we need to find both ϕ_0 and k_y, but in this paper we would fix ϕ_0, and just find k_y using a root-finding procedure. The series in (5) can be slowly convergent, so the leading asymptotic terms are extracted and summed with some fast convergent series, while the remaining part is summed directly, which, after this process, exhibits good convergence [10]. Notice that, when $k_y=0$, we have $K^{xy}=K^{yx}=0$, so the modes decouple into TE and TM waves, and k_{x0} is the eigenvalue to be found.

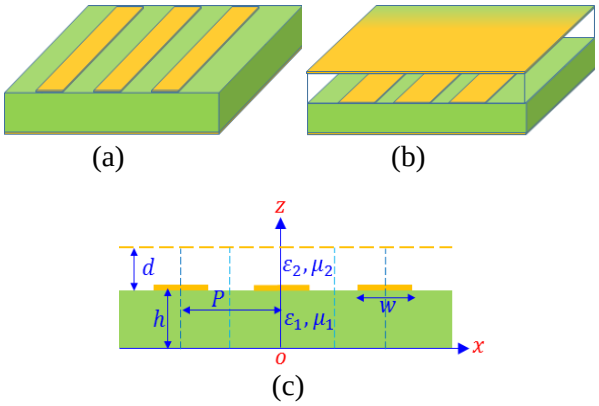

Fig. 1. Metal strip grating on grounded dielectric slab: (a) 3D view without top shield, (b) 3D view with top shield, and (c) edge view.

III. RELATIONS WITH PEC/PMC SHIELDED MICROSTRIPS

A. Symmetric case

Figure 2 shows the symmetric and non-symmetric shielded microstrips. On the two sides, the shields can be PEC walls, or PMC walls. The top shield may be absent when we consider their relationships with the MSG-GDS in Fig. 1 (a). Let's first consider the symmetric case. In the periodic structure, we place phase shift walls (PSWs) at the boundary of the first unit cell and obtain a shielded structure as well. The electric and magnetic fields for this structure can be expressed in Fourier series as:

$$\mathbf{F}(x,z)=\sum_{n=-\infty}^{\infty}\tilde{\mathbf{F}}(k_{xn},z)e^{-jk_{xn}x}, \quad (6)$$

where $\mathbf{F}\in\{\mathbf{E},\mathbf{H}\}$ and $\exp(-jk_y y)$ variation has been suppressed. In fact, the expressions for the fields in Fig. 2 are in the same form as (6), but the values of k_{xn} are different. Considering the mirror symmetry of the structure with respect to the yoz plane, one can classify the modes into two categories: even and odd [11]. To better under the parity of the modal fields, we first express the components of the spectral currents using the magnetic and electric vector potentials $\Phi_i^{(e)}$ and $\Phi_i^{(h)}$ as follows [12]:

$$\tilde{J}_x(k_{xn}) = jk_y^{-1}\begin{bmatrix}(k_2^2-k_y^2)\Phi_2^{(h)}(k_{xn},h)\\ -(k_1^2-k_y^2)\Phi_1^{(h)}(k_{xn},h)\end{bmatrix}$$

$$\tilde{J}_y(k_{xn}) = -jk_{xn}[\Phi_2^{(h)}(k_{xn},h)-\Phi_1^{(h)}(k_{xn},h)]$$

$$-\frac{\omega}{k_y}\frac{\partial}{\partial z}[\varepsilon_2\Phi_2^{(e)}(k_{xn},z)-\varepsilon_1\Phi_1^{(e)}(k_{xn},z)]_{z=h}, \quad (7)$$

where ω is the angular frequency and i indicates the i^{th} region. The above equations inform us that for a given mode, either even or odd, the currents in x and y directions have different parities in terms of k_x. Given the parity of a mode, parity of the current is specified, and then we can determine the parities of the potentials at the upper surface of the dielectric slab, which should be identical for all constant z planes. This would in turn allow us to identify the parities of all the components of the electric and magnetic fields. If we separately consider the two types of modes, and check the expressions for the electric and magnetic fields, we find that $\tilde{E}_y$ and $\tilde{E}_z$ have the same parity in terms of k_x, which differs from that of $\tilde{E}_x$; $\tilde{H}_y$ and $\tilde{H}_z$ have the same parity, but different from that of $\tilde{H}_x$. The parity of the fields in spectral domain, according to the properties of Fourier transform, is the same as that in spatial domain. With these in mind, we are ready to distinguish two types of modes, and define the modes as even modes if J_y, E_y, E_z, H_x are even and J_x, E_x, H_y, H_z are odd; the modes are odd modes if the converse is true. Now let's make use of (6), and examine the tangential fields at the PSWs ($x=\pm P/2$). For $\phi_0=0$, indicating the absence of phase shift between adjacent periods, we yield:

$$F_{y/z}(\pm P/2,z) = \tilde{F}_{y/z}(0,z)+\sum_{n=1}^{\infty}(-1)^n\begin{bmatrix}\tilde{F}_{y/z}(2n\pi/P,z)\\ +\tilde{F}_{y/z}(-2n\pi/P,z)\end{bmatrix}, \quad (8)$$

where $F\in\{E,H\}$. Obviously it vanishes if $F_{y/z}$ is an odd function of x. While for $\phi_0=\pi$, we acquire:

$$F_{y/z}(\pm P/2,z) = \mp j\sum_{n=0}^{\infty}(-1)^n\begin{Bmatrix}\tilde{F}_{y/z}[(2n+1)\pi/P,z]\\ -\tilde{F}_{y/z}[-(2n+1)\pi/P,z]\end{Bmatrix}, \quad (9)$$

which again vanishes if $F_{y/z}$ is even. The implication of the vanishing of tangential fields is that we can place PEC or PMC walls at the boundary and the modal profiles would remain unperturbed. Now if we take into account the parities of the modal fields as have been defined above, we conclude that the Periodic Boundary Condition (PBC) reduces to PEC boundary condition for the odd modes if $\phi_0=0$, for even modes if $\phi_0=\pi$; it reduces to PMC boundary condition for odd modes if $\phi_0=\pi$, for even modes if $\phi_0=0$. Think the other way around: Are all the modes of the PEC or PMC shielded microstrips included in the modes of the MSG-GDS with phase shift $\phi_0=0,\pi$? The answer is yes, because we can extend the domain of the PEC or PMC shielded structures to periodic ones by introducing infinite number of images according to the image theory. Then we are assured that the PEC and PMC boundary conditions are indeed special cases of the PBC for the symmetric structure under consideration. It should be noted that the above conclusions are not limited to the case when the strip thickness is 0, but also apply when the strips are of finite thickness, since our derivation only assumes mirror symmetry of the structure in this section and is independent of the zero-thickness assumption.

Since the structure is also mirror symmetric with respect to the plane $x=P/2$, we can also place PSWs at $x=0$ and $x=P$. Thus, a corresponding PEC or PMC shielded microstrip is obtained if PEC or PMC walls are placed. In this circumstance, the parity of a mode is defined in the same way as in the case for symmetry about $x=0$, but referred with respect to the central plane of the shielded microstrip at $x=P/2$. The modal relations between the three structures can be analyzed similarly. We tabulate the relations for both cases in Table 1. For the modes in the same row, they have the same propagation constant along the longitudinal direction. We can see that when $\phi_0=0$, the same walls are placed and the parities are the same for both symmetric cases, while when $\phi_0=\pi$, different walls are placed and the parities are opposite.

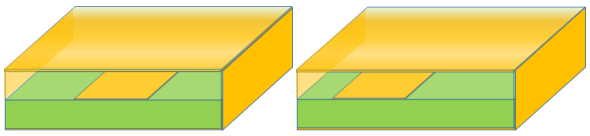

(a) (b)

Fig. 2. Shielded microstrips: (a) symmetric, and (b) non-symmetric.

Table 1: Summary of modal relations

	$x=0$ symmetry		$x=P/2$ symmetry	
$\phi_0=0$	PEC	Odd	PEC	Odd
	PMC	Even	PMC	Even
$\phi_0=\pi$	PEC	Even	PMC	Odd
	PMC	Odd	PEC	Even

B. Non-symmetric case

For non-symmetric case, the modes of the PEC/PMC shielded microstrips can no longer be divided into even and odd modes. But we can perform periodic extension in this case. As shown in Fig. 3 (a), where the arrows are used to illustrate the direction of current, we perform odd extension for the modes of PEC shielded microstrip, and all the modes of the original non-symmetric structure now correspond to the odd modes of the extended symmetric PEC shielded structure whose width has doubled. For the PMC shielded microstrip, we conduct even extension, and all the modes of the original structure has correspondence to the even modes of the extended structure. Now we make up a MSG-GDS with the extended structure in Fig. 3 (taking away the PEC or PMC walls) as the unit cell. Based on our previous discussions, we know the odd modes of the extended PEC shielded microstrip correspond to the modes with $\phi_0=0$ in the MSG-GDS (with extended unit cell), which means all the modes of the original non-symmetric PEC shielded microstrip correspond to the modes of MSG-GDS with $\phi_0=0$. Similarly, we have the correspondence between the modes of the non-symmetric PMC shielded microstrip and those of the MSG-GDS.

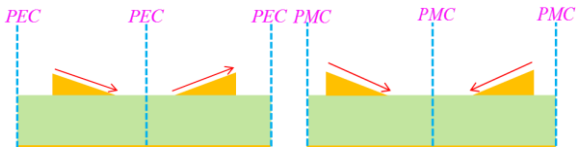

Fig. 3. Periodic extension for non-symmetric shielded microstrip: (a) PEC shielded, and (b) PMC shielded.

IV. NUMERICAL EXAMPLES

The first numerical experiment is about the PEC shielded microstrip as illustrated by Fig. 2 (a). Following the reference [13], we set the parameters as follows: $\varepsilon_{r1}=8.875$, $\mu_{r1}=1$, $\varepsilon_{r2}=\mu_{r2}=1$, $f=20$ GHz, $h=1.27$ mm, $w=h$, $d=11.43$ mm and $P=10h$. The first 5 modes are calculated and tabulated in Table 2, where the normalized wavenumbers are k_y/k_2. We can see that agreement of 8-10 digits is achieved, and we only use 4 terms in the expansion of the currents in x and y directions. It is to be noted that our results are obtained not by solving the eigenproblem of the shielded microstrip directly, but by solving that for the MSG-GDS. We pick up the modes of the shielded microstrip from the set of modes of MSG-GDS by letting $\phi_0=0$ or π and using basis functions with proper parites according to our previous conclusions. The good agreement achieved confirms our claims about the relationships between the MSG-GDS and shielded microstrip.

Table 2: Normalized wavenumbers in y direction

Mode	Reference [13]	Calculated
1 (even)	2.7102057109	2.7102057101
2 (odd)	1.2894527450	1.2894527434
3 (even)	1.1026365889	1.1026365888
4 (odd)	0.9223133480	0.9223133479
5 (even)	0.7250996002	0.7250996009

In practice, the shield for the microstrips may be used to model the packaging effect. Then one question arises: Which one captures the physics better, the PEC shielded microstrip, or the PMC shielded? So it is beneficial for us to compare the behavior of the two structures. Again, we do this by finding their eigen modes from a calculation of the MSG-GDS. Figure 4 shows the dispersion curves for the dominant modes of the PEC and PMC shielded microstrips in the range from 1 GHz to 25 GHz, where the effective permittivity is defined as the square of the normalized wave number. The parameters are: $\varepsilon_{r1}=9.7$, $\mu_{r1}=1$, $\varepsilon_{r2}=\mu_{r2}=1$, $w=1.219$ mm, $h=1.27$ mm and $P/w=5$. Here we assume there is no top shield. As indicated by the legend, both modes are even modes. It can be seen first that both effective permittivities increase with the frequency. Also, notice that the PMC shielded microstrip has a larger effective permittivity than the PEC shielded microstrip, and the difference between the two permittivities decreases with frequency and

eventually almost vanishes at high frequency. The reason for this is that the electromagnetic fields aggregate more in the vicinity of the metal strip, whose width is just 1/5 of the period. Therefore, we are grounded to treat the shields on both sides as far from the region where most energy rests, and it makes little difference whether we put a PEC or PMC wall.

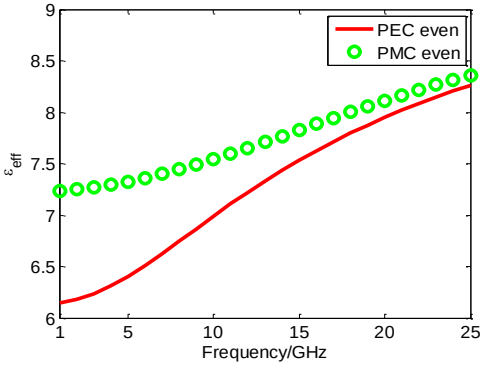

Fig. 4. Effective permittivity for the PEC/PMC shielded microstrip vs. frequency. Parameters: $\varepsilon_{r1}=9.7$, $\mu_{r1}=1$, $\varepsilon_{r2}=\mu_{r2}=1$, $w=1.219$ mm, $h=1.27$ mm and $P/w=5$.

In Fig. 5, the geometric parameters P, h, w are explored. Parameters common to Fig. 5 (a-c) are: $\varepsilon_{r1}=9.7$, $\mu_{r1}=1$, $\varepsilon_{r2}=\mu_{r2}=1$, $w=1.219$ mm. In Fig. 5 (a), w is very close to h, and the effective permittivities are plotted against the ratio P/w at 10 GHz. It is observed that the PMC shielded microstrip still has a larger effective dielectric constant than the PEC shielded microstrip, and the two permittivities approach each other when frequency is increased. At $P=1.5w$, the electric field distributions in the two structures are drawn in Fig. 6. The fields are calculated by convoluting the dyadic Green's function with the eigen-current, which can be found by solving (4) with the normalization that the l_2-norm of the expansion coefficients equals unity. The arrows in the graphs represent a snapshot of the vector fields, and color plot conveys the amplitude of the fields. It is very clear that the PEC shielded microstrip has the fields mostly confined around the two edges of the metal strip, and decays very quickly into the dielectric region and air region. Nevertheless, the PMC shielded microstrip drives most of the electric fields into the high dielectric region, and the distribution is also rather uniform. This implies that the PMC shielded microstrip in this configuration has a larger capacitance for storing electric energy, which is equivalently interpreted as a larger effective permittivity. But when P/w goes high, the PEC/PMC walls on both sides play a lesser role, which leads to very close effective permittivities.

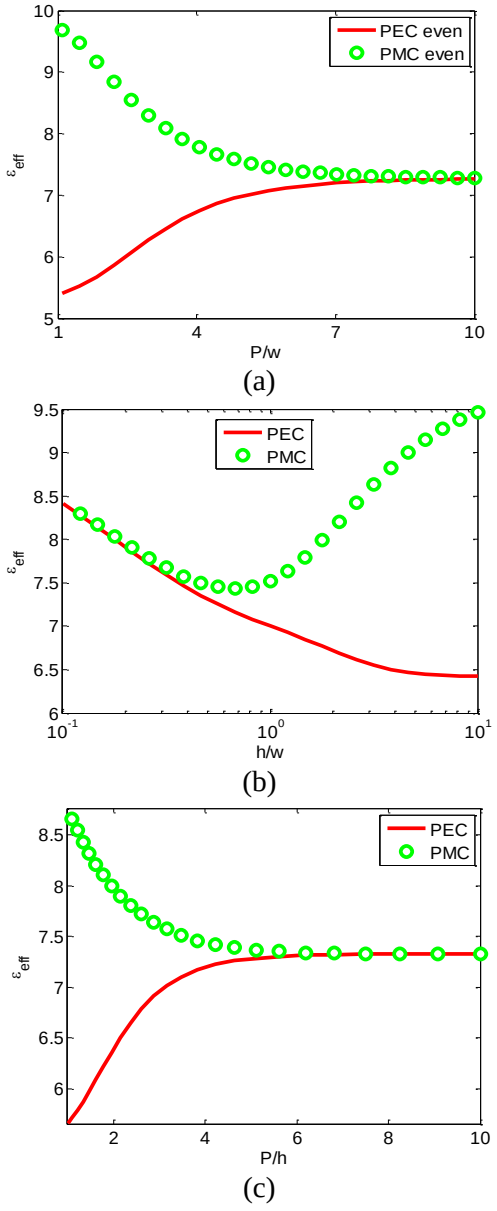

Fig. 5. Effective permittivity for the PEC/PMC shielded microstrip vs. geometry, with parameters: $\varepsilon_{r1}=9.7$, $\mu_{r1}=1$, $\varepsilon_{r2}=\mu_{r2}=1$, $w=1.219$ mm. (a) $h=1.27$ mm and $f=10$ GHz, (b) $f=10$ GHz and $P/w=5$, and (c) $h=5w$, and $f=5$ GHz.

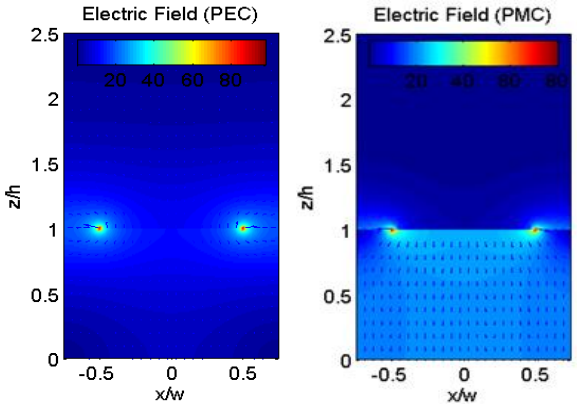

Fig. 6. Electric field (in V/m) distributions for PEC/PMC shielded microstrips. Parameters follow the two points at $P=1.5w$ in Fig. 5 (a).

The influence of the slab thickness is more complicated, as illustrated in Fig. 5 (b). For the PEC shielded microstrip, the effective permittivity keeps going down when the slab becomes thicker, while that for the PMC shielded microstrip descends to a valley before its rise. When h is very small, the two have almost the same effective permittivity. In this situation, we can think of a very thin parallel capacitor formed between the metal strip and the metal ground, and this capacitor has a large capacitance to store the energy in the small region near the metal strip. As a result, the fields can hardly reach the boundary on the two sides, shedding light on why the two permittivities are very close. For this point, we are confirmed by the field distribution in Fig. 7, where the field distributions for the two structures at $h=w$ are close to each other, and most of the fields are in the slab region. Besides, the fields decay to a very weak level at the PEC/PMC walls. When h is very large, the PMC shielded microstrip has a much larger effective permittivity than the PEC shielded microstrip. To make sense of this, we look at the (magnetic) field distributions at $h=10w$ in Fig. 8. We can see that for the PEC shielded microstrip, the fields decay away from the metal strip, but for the PMC shielded, things are different; there are peaks and valleys in the high dielectric region. The PMC shields influence the field distribution such that the mode is very close to a TEM wave in the slab region, and much more energy is stored in the slab. That is why it exhibits a larger dielectric constant.

In Fig. 5 (c), the dispersion curves of the PEC and PMC shielded microstrip are plotted against P/h, where $h=5w$ and $f=5$ GHz . Similar phenomena are observed as in Fig. 5 (a). From the above discussions, we are led to claim that the PMC shielded microstrip in general has a larger effective dielectric constant than the PEC shielded microstip, given that the frequency is not too high, the slab not too thin, and the width P is not significantly larger than the slab thickness h and strip width w.

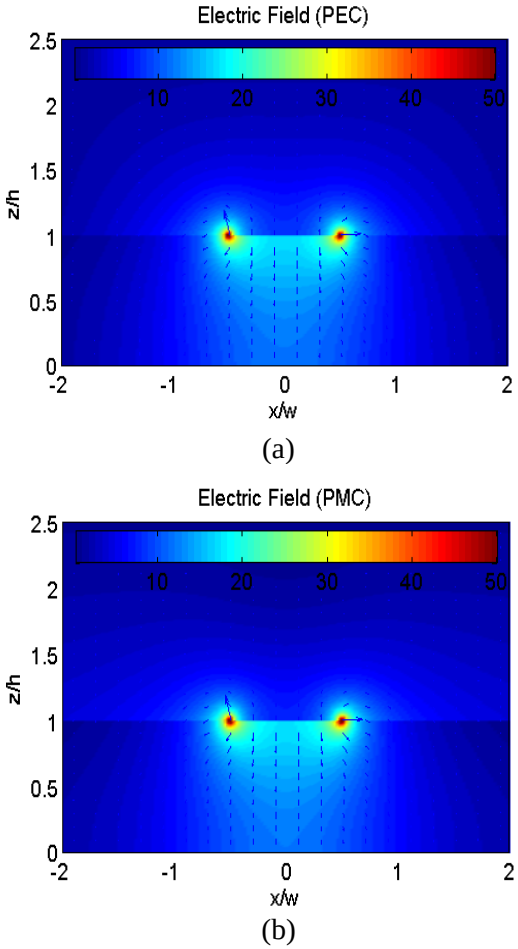

Fig. 7. Electric field (in V/m) distributions for PEC/PMC shielded microstrips. Parameters follow the two points at $h=w$ in Fig. 5 (b).

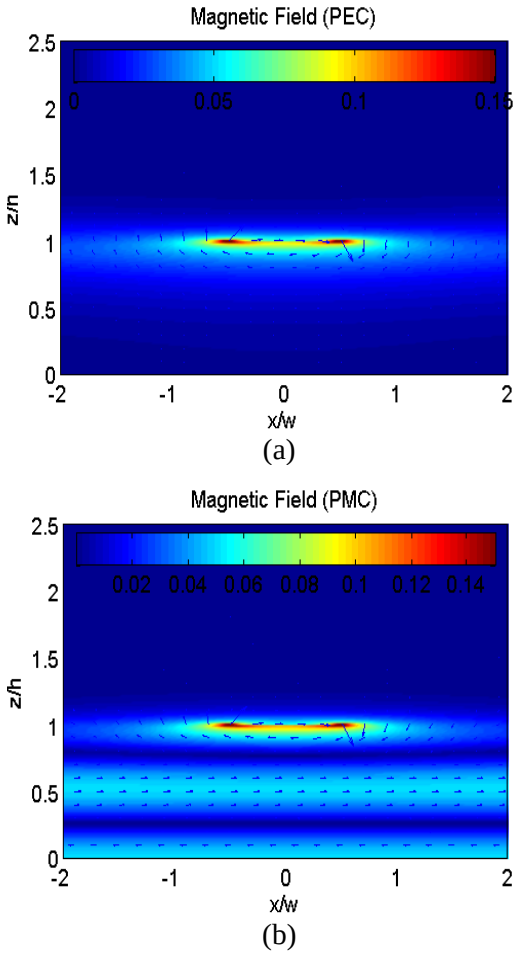

Fig. 8. Magnetic field (in A/m) distributions for PEC/PMC shielded microstrips. Parameters follow the two points at $h = 10w$ in Fig. 5 (b).

V. CONCLUSION

To summarize, this paper has investigated the modal relationships between Metal Strip Grating on Grounded Dielectric Slab (MSG-GDS) and PEC/PMC shielded microstrip by virtue of full wave spectral domain approach. By exploring symmetry of these structures and examining the tangential fields at the boundary, we have found that the PEC and PMC boundary conditions are special cases for the periodic boundary conditions. To be specific, it has been revealed and verified that all the even and odd modes of the mirror symmetric PEC/PMC shielded microstrip find their correspondence in the modes of metal strip grating on grounded dielectric slab when the phase shift between adjacent two unit cells is 0 or π. By performing a periodic extention for the non-symmetric shielded structures and making up a new MSG-GDS, all the modes for the original non-symmetric shielded structures also correspond to those of the MSG-GDS with 0 or π phase shift between adjacent unit cells. Through a calculation for the MSG-GDS and the use of the relations between the PEC/PMC shielded microstrips and MSG-GDS, we conduct a comparison of the PEC and PMC shielded microstrips. The effect of frequency and geometric parameters on the dominant modes for the PEC and PMC shielded microstrips have been studied. We found that the dominant (even) mode of the PMC shielded microstrip has in general a larger effective dielectric constant than the dominant (even) mode of the PEC shielded microstrip, due to a stronger capacity to drive more electromagnetic energy into the high dielectric region.

ACKNOWLEDGMENT

This work was supported in part by the Intel Corporation and the National Science Foundation CAREER Grant ECS-0547161.

REFERENCES

[1] S. Rakheja and A. Naeemi, "Interconnects for novel state variables: performance modeling and device and circuit implications," *IEEE Trans. Electron. Devices*, vol. 57, no. 10, pp. 2711-2718, 2010.

[2] W. C. Chew, "Waves and fields in inhomogeneous media," *IEEE Press*, New York, 1995.

[3] A. A. Melcón and J. R. Mosig, "Two techniques for the efficient numerical calculation of the green's functions for planar shielded circuits and antennas," *IEEE Trans. Microwave Theory Tech*., vol. 48, no. 9, pp. 1492-1504, 2000.

[4] R. E. Collin and F. J. Zucker, "Antenna theory," *McGraw-Hill*, New York, chapters 19-20, 1969.

[5] C. P. Nehra, A. Hessel, J. Shmoys, and H. J. Stalzer Jr., "Probe-fed strip-element microstrip phased arrays: E- and H-plane scan resonances and broadbanding guidelines," *IEEE Trans. Antennas Propag*., vol. 43, no. 11, pp. 1270-1280, November 1995.

[6] N. K. Das and A. Mohanty, "Infinite array of printed dipoles integrated with a printed strip grating for suppression of cross-polar radiation. part I: rigorous analysis," *IEEE Trans. Antennas Propag*., vol. 45, no. 6, pp. 960-972, June 1997.

[7] P. Baccarelli, P. Burghignoli, F. Frezza, A. Galli, P. Lampariello, G. Lovat, and S. Paulotto, "Modal properties of surface and leaky waves propagating at arbitrary angels along a metal strip grating on a grounded slab," *IEEE Trans. Antennas Propagat*.,

vol. 53, no. 1, pp. 36-46, 2005.

[8] K. Chen, J. M. Song, and T. Kamgaing, "Modal relationship between PEC/PMC shielded interconnect and grounded dielectric slab loaded with periodic metal strips," *Annual Review of Progress in Applied Computational Electromagnetics*, Monterey, CA, pp. 904-909, March 2013.

[9] T. Itoh, "Numerical techniques for microwave and millimeter-wave passive structures," *Wiley*, New York, NY, 1989.

[10] S. Jain, J. M. Song, T. Kamgaing, and Y. Mekonnen, "Acceleration of spectral domain approach for generalized multilayered shielded microstrip interconnects using two fast convergent series," *IEEE Trans. Components, Packaging, Manufacturing Tech.*, vol. 3, no. 3, pp. 401-410, 2013.

[11] J. D. Joannopoulos, S. G. Johnson, J. N. Winn, and R. D. Meade, "Photonic crystals: molding the flow of light," (second edition), chapter 3, *Princeton University Press*, Princeton and Oxford, 2008.

[12] R. Mittra and T. Itoh, "A new technique for the analysis of the dispersion characteristics of microstrip lines," *IEEE Trans. Microwave Theory Tech.*, vol. 19, no. 1, pp. 47-56, 1971.

[13] J. L. Tsalamengas and G. Fikioris, "Rapidly converging spectral-domain analysis of rectangularly shielded layered microstrip lines," *IEEE Trans. Microwave Theory Tech*., vol. 51, no. 6, pp. 1729-1734, 2003.

Kun Chen received the B.S. degree from The University of Electronic Science and Technology of China, Chengdu, China. He is currently pursuing the Ph.D. degree at Iowa State University. His current research interests are integral equation methods for electromagnetics and elastics, and non-destructive evaluation.

Jiming Song received the B.S. and M.S. degrees in Physics from Nanjing University, China, in 1983 and 1988, respectively, and the Ph.D. degree in Electrical Engineering from Michigan State University, East Lansing, in 1993.

From 1993 to 2000, he worked as a Postdoctoral Research Associate, a Research Scientist and Visiting Assistant Professor at The University of Illinois at Urbana-Champaign. From 1996 to 2000, he worked as a Research Scientist at SAIC-DEMACO. He was the Principal Author of the Fast Illinois Solver Code (FISC), which has been distributed to more than 400 government and industrial users. From 2000 to 2002, he was a Principal Staff Engineer/Scientist at Digital DNA Research Lab., Semiconductor Products Sector of Motorola, Tempe, Arizona. In 2002, he joined the Department of Electrical and Computer Engineering, Iowa State University, Ames, as an Assistant Professor and is currently an Associate Professor. His research has dealt with modeling and simulations of interconnects on lossy silicon and RF components, wave scattering using fast algorithms, wave propagation in metamaterials, and transient electromagnetic field. He has co-edited one book and published seven book chapters, 55 journal papers and 146 conference papers.

Song received the NSF Career Award in 2006 and the Excellent Academic Award from Michigan State University in 1992. He is an IEEE Fellow and was selected as a National Research Council/Air Force Summer Faculty Fellow in 2004 and 2005.